

# Thermal Sensitivity Analysis of a Telemetry Antenna in Sub-Orbital Spaceflights

Mahmoud Talafi Noghani<sup>1\*</sup>, Mohammad Nadjafi<sup>1</sup>

1. Aerospace Research Institute, Ministry of Science, Research and Technology, Tehran, Iran

\*[mtnoghani@ari.ac.ir](mailto:mtnoghani@ari.ac.ir)

## Abstract

A thermal sensitivity analysis is performed for an Inverted-F antenna (IFA) at the worst-case thermal condition (reentry phase) of a typical sub-orbital sounding-rocket spaceflight. Electromagnetic simulations show that a 300 Celsius change in the IFA temperature, mainly caused by the aerodynamic heating, increases the reflected power by 1% and decreases the antenna gain by 2.5%. The results show that the degradation of antenna performance and the telemetry link quality is negligible. Therefore, the IFA is a good antenna choice for similar sounding rockets from the thermal reliability point of view.

Keyword: Antenna; Inverted-F antenna; Thermal sensitivity analysis; Aerodynamic heating; Electromagnetic simulation

## 1. Nomenclature and Units

$\alpha_L$	Linear thermal expansion coefficient
$\sigma$	conductivity
$dB$	decibel
$d_{gap}$	gap length
$\Delta x$	displacement value
$\Delta L_V$	vertical length change
$\Delta L_H$	horizontal length change
$\epsilon_r'$	real part of permittivity
$\epsilon_r''$	imaginary part of permittivity
$H_t$	tangential magnetic field
$L_0$	length at $T_0$
$P_{LC}$	power loss in the conductor
$P_{Ld}$	power loss in dielectric
$R_s$	surface resistance
$S_{11}$	Reflection coefficient
$T$	temperature
$T_0$	reference temperature
$\tan\delta$	loss tangent
$HFSS$	High Frequency Simulation Software
$PTFE$	Polytetrafluoroethylene
$IFA$	Inverted-F Antenna
$MHz$	Mega Hertz
$RF$	Radio Frequency
$FEM$	Finite Element Method

## 2. Introduction

Reliability One of the known challenges in space missions is the thermal effects, especially on the outer

surface of spacecraft. Satellites experience a wide range of temperature changes (from about  $-150^{\circ}C$  to  $70^{\circ}C$ ) as they move from the bright side of the orbit (under direct sunlight) to the dark side (under earth's shadow) [1]. The potential effects of this temperature change on satellite subsystems must be predicted and analyzed in different development phases such as design, simulation, test, and verification[2-4].

This issue is more crucial for spacecrafts since they must survive the thermal tensions caused by the motion in the dense part of the atmosphere during the ascent and the reentry phases of the mission, and the thermal effects due to direct radiations. In sub-orbital sounding-rockets with supersonic speeds, aerodynamic heating is the main cause of temperature change [5]. Aerodynamic heating is the heating of a body produced by the passage of air (or gas) over it. It is caused by friction and compression processes and is significant chiefly a thigh speeds.

Antennas are the key elements in any space communication system, including sounding-rockets. They are directly affected by aerodynamic heating since their physical and electromagnetic characteristics require them to be mounted on the outermost surface of the rocket. Therefore, sounding-rocket antennas are designed and fabricated so that the aerodynamic heating does not affect the electromagnetic radiation characteristics considerably. Nevertheless, the aerodynamic heating and pressure are sometimes so high that the usage of the heat-resistant radome is inevitable.

Consequently, an important step in sounding-rocket antenna design is thermal sensitivity analysis.

Sensitivity analysis is a technique in determining the importance of choosing an analysis model based on its parameters, performance of particular variables, their severity, and the importance of each [6]. Sensitivity analysis is a routine and straightforward framework for any process [7,8]. In this regard, the effects of each input parameter on the output variables are investigated along with the accounting assumptions [9]. Each of the factors, folds, assumptions, and magnitude that can lead to the greatest change in the output variable value, are marked as sensitive parameters and must be analyzed to demonstrate their significance [10]. This analysis highlights the elements and factors that are the main sources of change. It also evaluates the quality of the proposed model and research results.

In the field of sensitivity analysis with applications for aerospace systems, few studies have been conducted. The effects of conductive heat transfer due to solar radiation and the surrounding environment on a spacecraft have been investigated for thermal sensitivity [11]. The effects of various parameters on the useful life of the spacecraft battery have been investigated. In another study, sensitivity analysis based on probability theory for modeling spacecraft and space debris was investigated and, in addition to extracting mathematical equations to cover the aerothermodynamic properties of cubic and cylindrical space objects, heat flux distribution on the shell of these objects has also been developed [12]. Recently, to design space systems, an intelligent strategy has been developed to be able to optimize the thermal design of the spacecraft based on statistical machine learning and the ability to analyze thermal sensitivity on all surfaces of the device [13].

This paper aims to perform the thermal sensitivity analysis of an Inverted-F antenna (IFA) mounted on a sounding-rocket body. The antenna is used to send the telemetry data gathered from atmospheric measurement instruments. This is based on an aerodynamic heating analysis similar to the one performed in [14]. This work considers the internal and external heating sources, and their corresponding temperature increases are worked out. Temperature-sensitive electromagnetic and physical parameters of the metallic and the dielectric parts of the antenna are presented, and the effect of temperature increase on the antenna performance is calculated and discussed. The results show that the designed IFA is quite insensitive to aerodynamic heating in the presumed conditions and suitable for the mission, as mentioned earlier.

The remainder of this paper is structured as follows: Section 2 presents the structure of the Inverted-F antenna used in the sounding-rocket (as a case study in this research), its generalities, and geometry. Method of analysis is provided in section 3, in which the sources of

heat and the characteristics of the temperature-dependent parameters are presented. In section 4, the results are provided, and the discussion is presented. The paper ends with the concluding remarks.

### 3. Inverted-F Antenna Structure

The structure of an Inverted-F antenna and its orientation on a typical sounding-rocket is depicted in Figure 1. Dimensions are given for an impedance-matched L-band (930MHz) telemetry antenna. The antenna structure is composed of a metallic body made from Brass and plated with Nickel-Chrome and an excitation region filled with Polytetrafluoroethylene (PTFE) dielectric material. The antenna is mounted on an Aluminium cylindrical shell, accounted as the rocket body.

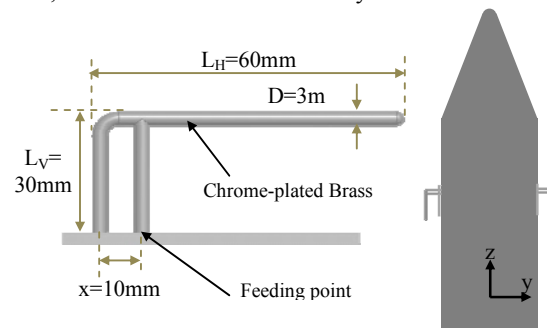


Figure 1. Geometry of an L-band, Inverted-F antenna for sounding-rocket telemetry transmission

### 4. Method of Analysis

The basic steps which can be used to analyze the sensitivity in the current case are given in the flowchart in Figure 2.

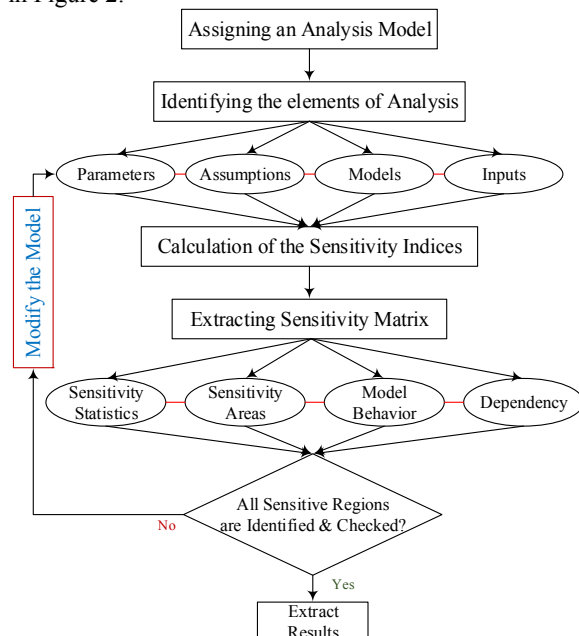


Figure 2. Basic sensitivity analysis steps

In the first step, one must define a model for the analysis.

This might depend on the problem conditions and the required accuracy. Accordingly, the elements of analysis are identified. These include the problem assumptions, sensitive parameters, variable inputs, and the physical models considered. The models depend on the nature of the problem. It could be a purely theoretical model based on mathematical descriptions or a numerical model depending on the complexity of the physical characteristics. Following, the sensitivity indices are calculated, and the matrices are extracted. These unveil the relative importance and classification of parameters (sensitive statistics) and their sensitive regions, probable unusual model behavior, and the parameter dependency (if required, through correlation and regression analysis).

The sensitivity analysis results may be used to identify areas where more data collection and better analysis are required (for example, using higher and more accurate techniques and models) [15]. Based on the flowchart of Fig. 2., after checking and identifying acceptable ranges of results, if the results are not within the acceptable region, corrective changes must be made to the system and the results recalculated. A sensitivity analysis can be performed to identify the factors that predominate in the system's unreliability [16]. It should be noted that reducing the sources of human error or redesigning protection systems can improve system performance.

The accuracy and reliability of the output indicate the usefulness of a model. Studying the outputs of the uncertainty of an output parameter resulting from modeling, analyzing, and simulating a system and accessing various sources of uncertainty in input variables is one of the achievements of the study of sensitivity analysis [17].

The antenna thermal analysis in a sounding-rocket is an aero-thermo-electromagnetic analysis in which the coupled equations of aerodynamics, thermodynamics, and electromagnetics should be incorporated. Heat is generated by both aerodynamic and electromagnetic sources and affects the antenna temperature through thermodynamic laws. The increase in the antenna temperature (T: analysis input parameter) changes its physical size and electromagnetic parameters including the conductivity, permittivity, and loss, and finally alters the electromagnetic radiation characteristic of the antenna (analysis output parameters). It should be noted that, although not critical in the current case, the change in conductivity and permittivity of materials, alters the internal electromagnetic heat generation.

A complete solution that requires a multi-physics platform to solve the three aforementioned coupled equations simultaneously, is very complex, time-consuming, and almost impractical. From an engineering point of view, it is sufficient to know the steady-state results in the worst case. The transient response of this complex system might be of minor

interest, provided that the worst case is well below the critical region of the antenna characteristics. Therefore, the analysis presented here consists of two independent steps. Firstly, the heat sources are identified, and a suitable analysis is performed to calculate approximately the maximum possible temperature ( $T_{max}$ ) that the IFA reaches. Secondly, temperature-dependent electromagnetic parameters of the IFA and their corresponding relations are introduced. Then, a full-wave 3D electromagnetic simulation tool (High-Frequency Simulation Software (HFSS)) is used to calculate the IFA radiation properties at the desired temperatures, including  $T_{max}$ .

#### 4.1 Sources of Heat

Generally, there are two sources of heat: 1. Internal and 2. External. The internal source includes: a. the heat generated from the power dissipation at the RF front end components (especially power amplifiers), b. the energy dissipated in the metallic and the dielectric part of the antenna upon power injection, described as follows:

*Metal conduction loss:* it is the RF power loss due to the flow of electric current through the metal, mainly in the skin depth region near the surface, and is calculated as:

$$P_{LC} = \frac{R_s}{2} \int_s |H_t|^2 ds \quad ; \quad R_s = \sqrt{\frac{\omega \mu_0}{2\sigma}} \quad (1)$$

$R_s$  is the surface resistance of the metal, and  $H_t$  is the tangential magnetic field component. Conduction loss is inversely proportional to the conductivity ( $\sigma$ ) of metal.

*Dielectric energy loss:* it is the electromagnetic energy absorption at the molecule level inside the dielectric material and is calculated as:

$$P_{Ld} = \frac{\omega \epsilon_0 \epsilon_r''}{2} \int_V |E|^2 dV \quad (2)$$

Where  $\epsilon_r''$  is the imaginary component of the dielectric function and represents the material loss. The material loss is also shown by loss tangent ( $\tan \delta$ ), which is related to  $\epsilon_r''$  by  $\tan \delta = \epsilon_r'' / \epsilon_r'$ , where  $\epsilon_r'$  is the real part of the dielectric function.

In a typical sub-orbital mission, the power transmitted to telemetry antennas is at most a few tens of watts (30 W in our case study). For the specified IFA, the sum of  $P_{LC}$  and  $P_{Ld}$  is less than 100mW, so the related heat generation is negligible. Assuming a linear power amplifier with an efficiency of 20%, the power loss would be 120 W. This would lead to a temperature increase of about 40°C in the PA box. The generated heat will reach the IFA through a power divider, RF connectors, and cable increasing by less than 5°C in the IFA.

The External sources of heat are a. solar heating (direct sunlight), b. infrared radiation from the earth, c. earth albedo (solar reflection) heating, and d. aerodynamic heating. The solar or IR radiations are not of much concern in sub-orbital missions because the

rocket is subject to direct radiations for a very short period. Therefore, we should focus on aerodynamic heating.

In aerodynamic heating, the increase in surface temperature is approximately proportional to the square of speed. This heating is prominent at supersonic speeds. Predicting the surface temperature requires the coupled solution of the flow field governing equations and solid phase energy equation. Since such simulations are very time-consuming, methods based on decoupling the flow field and the solid phase governing equations could be used. According to the analysis presented in [14], suitable equations could compute the heat flux during supersonic flight. Then the one-dimensional heat conduction distribution in the solid phase could be used to predict the surface temperature variation of the rocket body.

In this regard, the results of an aerodynamic heating analysis similar to [14] will be used by assuming a typical geometry, a supersonic sounding-rocket payload that has the highest thermal flux when its thermal current is about 5 Mach in the reentry phase.

Thermal analysis is performed by assuming that the rocket body is composed of an aluminum metallic shell of the thickness of 3mm, and it is filled with a thermal insulator. The temperature change of the outer surface versus time is depicted in Figure. 3. It is shown that the maximum temperature of the rocket surface reaches about T= 300°C (573.2°K) near the IFA element outer body. Adding the value of temperature rise due to the internal sources, the maximum temperature of the IFA would be less than T = 600°K, which we will take into account throughout the analysis.

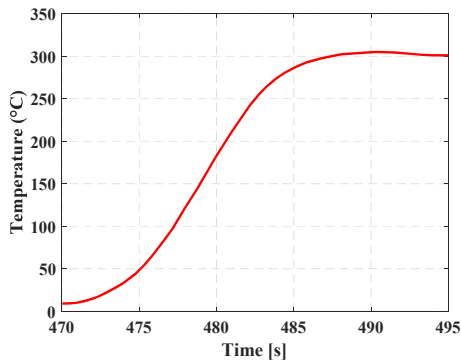


Figure 3. Surface temperature change versus time in the reentry phase of a sounding-rocket

### 4.2 Modeling The Temperature-Dependent Parameters

Temperature change occurring in the antenna will affect the following sensitive parameters: 1. Metallic Conductivity ( $\sigma$ ), 2. Dielectric Loss tangent ( $\tan \delta$ ), 3. Dielectric permittivity ( $\epsilon_r$ ), 4. Material Thermal expansion coefficient ( $\alpha$ ) and 5. Antenna size.

Using the mathematical thermal models introduced in [18-22], these parameters are formulated as follows:

$$\sigma_{Cr} = \frac{1}{1.6 \times 10^{-14} T^3 - 8.6 \times 10^{-12} T^2 + 2.6 \times 10^{-9} T - 2.0 \times 10^{-7}} \quad (3)$$

$$\sigma_{Al} = \begin{cases} (-1.5 \times 10^{-15} T^3 + 8.2 \times 10^{-13} T^2 - 1.8 \times 10^{-11} T + 1.4 \times 10^{-8})^{-1} & 0 < T < 300K \\ 2.6 \times 10^{13} T^{-2.78} + 2.1 \times 10^7 & 300 < T < 600K \end{cases} \quad (4)$$

$$\epsilon_{r, PTFE} = -7.1 \times 10^{-7} T^2 - 7.1 \times 10^{-5} T + 2.1 \quad (5)$$

$$\tan \delta_{PTFE} = -3.0 \times 10^{-9} T^2 + 3.6 \times 10^{-6} T - 5.8 \times 10^{-4} \quad (6)$$

$$\alpha_{L, Brass} = 9.9 \times 10^{-9} T + 16.9 \times 10^{-6} (1/^\circ K) \quad (7)$$

T is in Kelvin. The plotted curves of Eq. (3) - (7) are depicted in Fig. 4-6.

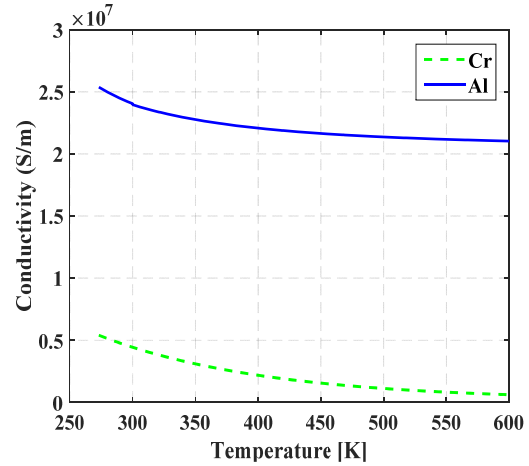


Figure 4. Metallic Conductivity ( $\sigma$ )vs. temperature ( $^\circ K$ ) [18]

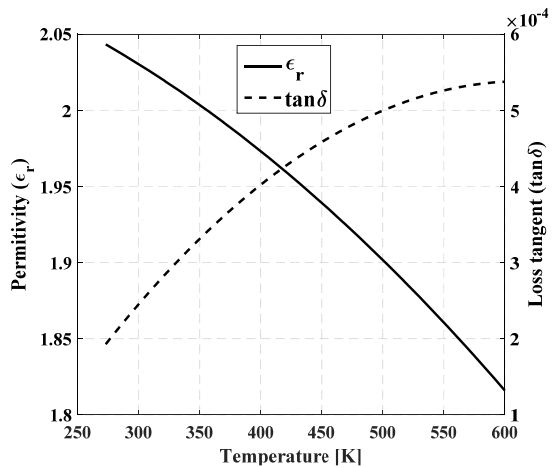
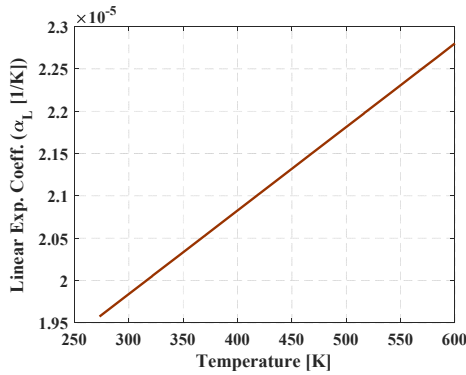
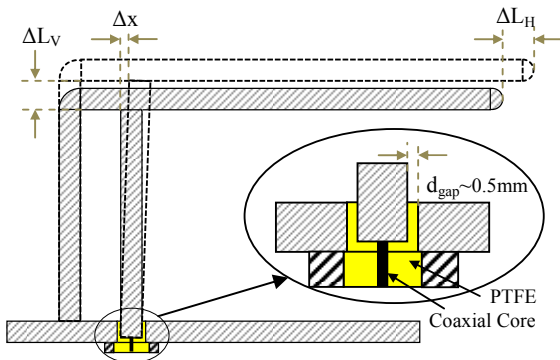


Figure 5. Permittivity ( $\epsilon_r$ )and loss tangent ( $\tan \delta$ ) vs. temperature ( $^\circ K$ ) for PTFE [19-20]



**Figure 6.** The linear thermal expansion coefficient of Brass ( $\alpha_L$ ) vs. temperature ( $^{\circ}\text{K}$ ) [21-22]

At the frequency of operation, the skin depth of the metal is about  $8\mu\text{m}$ . Since the chrome plating would be thicker than this depth, we can model the IFA metallic loss with chrome conductivity. Although heat expands all of the antenna dimensions (diameter and length), we consider the length expansion in our calculations because 1. The ratio of the overall antenna length to its diameter is high ( $>20$ ), so the length expands much more than the diameter, 2. Radiation characteristics of resonant wire antennas like IFA are much more sensitive to the change in length than the change in thickness. Metals have lower conductivity in higher temperatures, as is depicted in Fig. 4. So their loss increases with a temperature rise. This is the same for the PTFE loss tangent (Fig. 5). It increases by an amount of 35% when the temperature increases from 273 to  $600^{\circ}\text{K}$ . The thermal coefficient ( $\alpha$ ) also increases (linearly) with temperature shows that metals tend to expand more in higher temperatures (Fig. 6). The permittivity of PTFE decreases by 10% in the mentioned temperature range. This could affect the antenna input reflection coefficient, as is discussed in the next section.



**Figure 7.** Cross-section of the feeding point and the change in the geometry of IFA upon temperature rise

The IFA fixture is in a way that the left rod is fixed to the ground basis, and the right rod is connected to the core of the feeding coaxial cable, and it is separated from the ground basis by a dielectric (PTFE) filling (Fig. 7). When the IFA is exposed to heat, one can assume that the horizontal part lengthens rightward and the left rod lengthens upward. The right rod moves, as is shown in Fig.

7. The new lengths of each of these two parts can be calculated using:

$$L = L_0 + \Delta L; \quad \Delta L = L_0 \alpha_L \Delta T \quad (8)$$

$L_0$  is the length at  $T_0$ , which is the reference temperature (normally  $300^{\circ}\text{K}$ ).

According to the steps depicted in Fig. 2, the analysis parameters, models and assumptions are ready to perform the sensitivity calculations.

## 5. Results and Discussion

The linear thermal expansion coefficient of Brass and the related dimension value changes of the IFA are calculated using Eq. (7) and (8) for  $T=300^{\circ}\text{K}$  (the reference room temperature of  $23^{\circ}\text{C}$ ) and  $T=400, 500,$  and  $600^{\circ}\text{K}$  (maximum surface temperature) and are shown in Table 1. It should be noted that the displacement value of the right rod ( $\Delta x < 0.1\text{mm}$ ) is well below the gap length ( $d_{\text{gap}} \sim 0.5\text{mm}$ ). This assures that no short circuit occurs on the feeding point.

**Table 1.** Values of Linear Thermal Expansion of Brass and IFA Length changes at Different Temperatures

T ( $^{\circ}\text{K}$ )	$\alpha_L$ ( $10^{-6}/^{\circ}\text{K}$ )	Dimension Changes (mm)		
		$\Delta L_H$	$\Delta L_V$	$\Delta x$
300	19.84	0	0	0
400	20.83	0.12	0.06	0.02
500	21.81	0.26	0.13	0.04
600	22.80	0.41	0.21	0.07

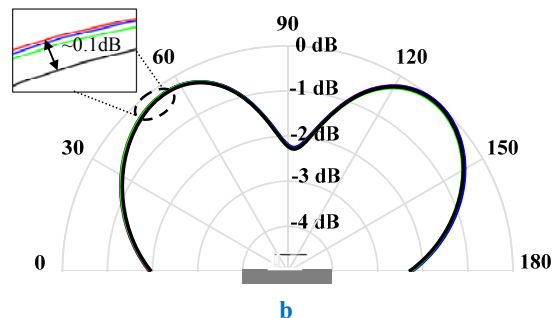
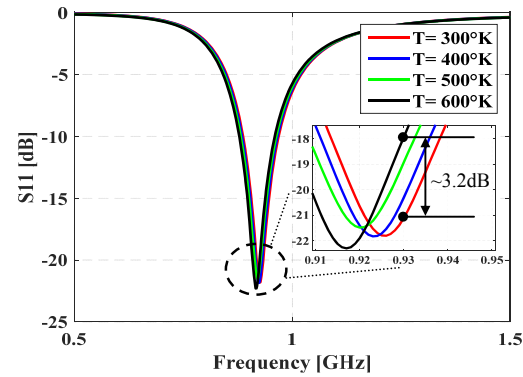


**Figure 8.** The IFA simulation results: **a.** input reflection coefficient (S11), **b.** radiation pattern.

Conductivities, dielectric permittivity, and loss tangent are calculated using Eq. (3) – (6) and are shown in Table 2.

**Table 2.** Values of IFA Electromagnetic Parameters at Different Temperatures

T (K)	Chrome	aluminum	PTFE	
	$\sigma$ (*10 <sup>7</sup> )	$\sigma$ (*10 <sup>7</sup> )	$\epsilon_r$	$\tan\delta$
300	0.44	2.40	2.03	0.00024
400	0.22	2.21	1.97	0.00040
500	0.11	2.14	1.90	0.00050
600	0.06	2.10	1.82	0.00054

A single IFA mounted on the cylindrical body of the sounding rocket is now simulated using the HFSS 3Delectromagnetic simulation software by the highly accurate finite element method (FEM) frequency-domain solver. Simulation is performed for the frequency range of 0.5-1.5 GHz. It is carried out for the temperatures and the corresponding parameters mentioned in Tables 1 and 2. The antenna input reflection coefficient ( $S_{11}$ ) and radiation pattern are calculated and the results are depicted in Fig. 8. The radiation pattern is plotted for the working frequency of 930 MHz. A rise of 300 Celsius degrees in IFA temperature has caused a change of 3.2 dB in  $S_{11}$ (Fig. 8-a) and 0.1dB in gain (Fig. 8-b). $S_{11}$  is still no more than -18dB, corresponding to a reflected power of 1.5%, and the antenna gain is just decreased by 2.5%. These changes have a negligible effect on the antenna performance, and the quality of the telemetry link is mainly retained, especially in the reentry phase of the mission. The results conclude that the analysis model used is suitable, and the assumptions are well within the acceptable limits of the antenna characteristics. There is no need to modify the model and repeat the process. Thus, the IFA is a good choice for a typical sounding-rocket sub-orbital mission from the thermal reliability point of view.

## 6. Conclusion

Aerodynamic heating is the main source of temperature rise on the surface of sub-orbital vehicles. This heat-up could degrade the performance of antennas on the outer surface of a sounding-rocket. Metal Conductivity ( $\sigma$ ), Dielectric permittivity ( $\epsilon_r$ ) and Loss tangent ( $\tan\delta$ ), Material Thermal expansion coefficient ( $\alpha$ ) and finally the antenna size are the sensitive parameters that are affected by this temperature rise. A two independently stepped analysis is presented here, in which the 3D electromagnetic simulation of the antenna is performed based on the steady-state results obtained from the thermally modified parameters. This simplified method could be used for similar problems where the worst-case thermal effects are intended. The thermal analysis performed for the assumed mission and based on the obtained results shows that a rise of 300 Celsius in temperature, caused mainly by aerodynamic heating, has negligible effects on the IFA

electromagnetic characteristics. Thus, it is a good choice for similar sounding-rockets.

## 7. References

- [1] F. Farhani and A. Anvari, "Effects of Some Parameters on Thermal Control of a LEO Satellite" *Journal of Space Science and Technology*, vol. 7, no. 1, pp. 13-24, 2014.
- [2] J. R. Tsai, "Overview of Satellite Thermal Analytical Model," *Journal of Spacecraft and Rockets*, vol. 41, no. 1, pp. 120-125, 2004.
- [3] A. Garzón, Y. A. Villanueva, "Thermal Analysis of Satellite Libertad 2: A Guide to CubeSat Temperature Prediction," *Journal of Aerospace Technology and Management*; <https://doi.org/10.5028/jatm.v10.1011>.
- [4] F. Sadeghikia and F. Asdaghpour, "Thermal Effects of the Space Environment on the Radiation Characteristics of a Reflector Antenna in LEO Spacecrafts," *Journal of Space Science and Technology*; <https://doi.org/10.30699/JSST.2021.258362.1316>
- [5] C. J. Riley F. R. Dejarnette, "Engineering aerodynamic heating method for hypersonic flow," *Journal of Spacecraft and Rockets*, vol. 29, no. 3, pp. 327-339, 1992.
- [6] A. Saltelli, "Sensitivity analysis for importance assessment," *Risk analysis*, vol. 22, no. 3, pp. 579-590, 2002.
- [7] H. C. Frey, and S.R. Patil, "Identification and Review of Sensitivity Analysis Methods," *Risk analysis*, vol. 22, no. 3, pp. 553-578, 2002.
- [8] D.A. Tortorelli, and P. Michaleris, "Design sensitivity analysis: overview and review," *Inverse problems in Engineering*, vol. 1, no. 1, pp. 71-105, 1994.
- [9] S. Abdollahi, and M.S. Rad, "Reliability and Sensitivity Analysis of a Batch Arrival Retrial Queue with k-Phase Services, Feedback, Vacation, Delay, Repair and Admission," *International Journal of Reliability, Risk and Safety: Theory and Application*, vol. 3, no. 2, pp. 27-40, 2020.
- [10] D. M. Hamby, "A review of techniques for parameter sensitivity analysis of environmental models," *Environmental monitoring and assessment*, vol. 32, no. 2, pp. 135-154, 1994.
- [11] S. Suresha, S. Gupta, and R. Katti, "Thermal sensitivity analysis of spacecraft battery," *Journal of spacecraft and rockets*, vol. 34, no. 3, pp. 384-390, 1997.
- [12] P. M. Mehta, et al. "Sensitivity analysis towards probabilistic re-entry modeling of spacecraft and space debris," *AIAA Modeling and Simulation Technologies Conference*. Florida, 2015.
- [13] Y. Xiong, et al., "Intelligent optimization strategy based on statistical machine learning for spacecraft thermal design," *IEEE Access*, vol. 8, pp. 204268-204282, 2020.
- [14] A. M. Tahsini, S. A. Hosseini, "An Accurate Prediction of Surface Temperature History in a Supersonic Flight," *International Journal of Mechanical and Mechatronics Engineering*, vol.7, no.12, 2013.
- [15] R. tejaNallapu, and J. Thangavelautham, "Design and sensitivity analysis of spacecraft swarms for planetary moon reconnaissance through co-orbits," *Acta Astronautica*, vol. 178, pp. 854-869, 2021.
- [16] H. Karimaei, "Sensitive Analysis of Tuned Mass on High Cycle Fatigue Safety Factor of Crankshaft," *International Journal of Reliability, Risk and Safety: Theory and Application*, vol. 3, no. 1, pp. 61-67, 2020.

- [17]M. Nadjafi, F. Ommi, and M.A. Farsi, "Uncertainty Analysis of Spray Injection Process in a Model Scale Liquid Fuel Micro-Motor," *Iranian Journal of Mechanical Engineering Transactions of the ISME*, vol. 21, no. 2, pp. 14-32, 2020.
- [18]COMSOL Multiphysics Simulation Software Ver. 4.2, Material Database.
- [19]B. Riddle, J. B. Jarvis, and J. Krupka, "Complex Permittivity Measurements of Common Plastics Over Variable Temperatures," *IEEE Transactions On Microwave Theory and Techniques*, vol. 51, no. 3, March, 2003.
- [20]P. Ehrlich, "Dielectric Properties of Teflon from Room Temperature to 314° C and from Frequencies of 102to 105c/s," *Journal of Research of the National Bureau of Standards*, vol. 51, no.4, Research Paper 2449, 1953.
- [21]<http://aries.ucsd.edu/LIB/PROPS/PANOS/cu.html>.
- [22]D. R. Lide, *CRC Handbook of Chemistry and Physics, 88th edition*. Boca Raton: CRC Press, 2008.